Stem Cell Research & Therapy

RESEARCH

Open Access

CX43-mediated mitochondrial transfer maintains stemness of KG-1a leukemia stem cells through metabolic remodeling

Huihui Fu[1†], Xiaoqing Xie[1†], Liuyue Zhai[1], Yi Liu[1], Yifeng Tang[1], Sanxiu He[1], Jun Li[1], Qing Xiao[1], Guofa Xu[1,2], Zailin Yang[1*], Xiaomei Zhang[1*] and Yao Liu[1*]

Abstract

Background Acute myeloid leukemia (AML) is characterized by abundant immature myeloid cells, relapse and refractory due to leukemia stem cells (LSCs). Bone marrow mesenchymal stem/ stromal cells (BMSCs) supported LSCs survival, meanwhile, chemotherapy improved connexin43 (CX43) expression. CX43, as the most intercellular gap junction, facilitated transmit mitochondria from BMSCs into AML. We hypothesized that increased mitochondria transferred from BMSCs supported metabolic remodeling in LSCs to sustain their stemness.

Methods Primary BMSCs from AML patients were isolated. CX43-BMSCs, overexpressing CX43, were cocultured with KG-1a cells. Fluorescence and confocal microscopy observed mitochondrial transfer. Flow cytometry, EdU assay, and clonogenicity evaluated cell cycle, proliferation, and clonogenic potential. Xenograft mouse models were used to evaluate the tumorigenicity of KG-1a in vivo. Seahorse, RNA-seq, and LC-MS assessed mitochondrial function, transcriptomes, and metabolites post-coculture.

Results CX43-BMSCs promoted unidirectional mitochondrial transfer, enhancing KG-1a adhesion and proliferation to maintain LSCs stemness in vitro and vivo. RNA-seq revealed coculture with CX43-BMSCs upregulated genes related to adhesion, proliferation, and migration in KG-1a cells. Elevated CX43 expression strengthened BMSCs-KG-1a interaction, facilitating mitochondrial transfer and nucleoside metabolism, fueling KG-1a cells. This enhanced mitochondrial energy metabolism, promoting metabolic reprogramming and clonogenicity.

Conclusion CX43-mediated mitochondrial transfer from BMSCs to KG-1a enhances LSCs adhesion, proliferation, clonogenicity, and metabolic reprogramming. CX43 emerges as a potential therapeutic target for AML by sustaining LSCs stemness through metabolic remodeling.

[†]Huihui Fu and Xiaoqing Xie contributed equally to this work.

*Correspondence:
Zailin Yang
zailinyang@cqu.edu.cn
Xiaomei Zhang
20121901038@cqu.edu.cn
Yao Liu
liuyao77@cqu.edu.cn

Full list of author information is available at the end of the article

Keywords Leukemia stem cells, Bone marrow microenvironment, Connexin, Adhesion, Mitochondrial transfer, Metabolic remodeling

Introduction

Acute myeloid leukemia (AML) is a heterogeneous disease characterized by abundant immature myeloid cells in bone marrow, arresting the ability to leukocyte differentiation [1]. As the most popular form of adult acute leukemia, AML arises in different age groups, older patients who are more than 65 years old are the predominantly [2, 3]. Nearly two-thirds of adult patients relapsed followed by the first-line treatment or failed to achieve remission [4]. Advancing, the progression of molecular pathogenesis and treatment innovation has been highly improved, but it's still a big challenge for hematologists to treat relapsed or refractory patients effectively [5]. Quiescent leukemic stem cells (LSCs), which were thought the primary reason for relapse and refractory [6], to achieve long-term remission LSCs are urged to eradicate [7].

Bone marrow (BM) niche, also known as BM environment, is composed of mesenchymal stem/stromal cells (BMSCs), endothelial cells, osteoblasts, extracellular matrix proteins, and others [8]. BM niche is the location of hematopoietic stem and progenitor cells and contributes to self-renewal, differentiation, and survival of hematopoietic stem cells (HSCs) [9]. LSCs acquire many characteristics of HSCs, LSCs reliant on BM niche for survival and self-renewal. Altered metabolic programming happened in LSCs [10]. Moreover, recent studies indicated that LSCs possessed higher mitochondrial oxidative phosphorylation (OXPHOS) for their high metabolic demand than bulk AML cells [11]. Elevated levels of OXPHOS of LSCs were associated with chemotherapy resistance [12]. BMSCs could increase energy production in LSCs through increased TCA cycle and OXPHOS, contributing to AML development and chemoresistance [13]. The mechanism of how BMSCs provide LSCs with additional energy is not fully elucidated.

Connexin families play a pivotal role in intercellular communication between adjacent by forming gap junctions (GJICs), connexin43 (CX43) is the most current [14]. In addition to constituting GJICs, CX43 is also found in tunneling nanotubes (TNTs) [15]. CX43 was expressed between BMSCs and hematopoietic cells [16]. Functional GJICs in BMSCs has a direct impact on the proliferation and differentiation of hematopoietic stem/progenitor cells. The self-renewal and low immunogenicity of BMSCs was maintained by CX43 [17]. Our previous studies showed higher CX43 was expressed on BMSCs of post-chemotherapy compared with primary acute leukemia BMSCs [18]. Besides, CX43 helped BMSCs' mitochondrial transfer to nearby cells [19]. Mitochondrial transfer from BMSCs to LSCs may be one of the main mechanisms that BMSCs provided LSCs with additional energy. Here we hypothesize higher CX43 on BMSCs might support LSCs through mitochondria transfer and metabolic properties. We studied how the role of CX43-overexpression on BMSCs (CX43-BMSCs) influenced LSCs. CX43-BMSCs improved LSCs stemness. Because of the CX43 overexpression on BMSCs, more mitochondria were transferred from BMSCs to LSCs, LSCs get more locations to burn energy to improve OXPHOS level and maintain LSCs' survival and drug resistance. As OXPHOS was increased, amino acid uptake was increased through metabolite analysis.

Materials and methods

Sample acquisition and cell culture

Bone marrow aspirates were acquired from newly diagnosed AML patients, mononuclear cells were isolated by density gradient centrifugation with human bone marrow mononuclear cell isolation kit (Haoyang Biological Manufacture, Tianjin, China). 10^5 cells/cm^2 bone marrow mononuclear cells were plated with the human mesenchymal stem cell medium (7501, ScienCell, California, USA) plus mesenchymal stem cell growth supplement (7552, ScienCell, California, USA), 5% fetal bovine serum (70025, ScienCell, California, USA), 10000 U/mL penicillin, and 10000 μg/mL streptomycin (0503, ScienCell, California, USA). Adherent cells were collected and reseeded at a density of about 9000 cells/cm^2 until at least 4 generations. 4–5 passage BMSCs were used in experiments. KG-1a (acute myeloblastic leukemic cell line; ATCC) cultured with RPMI 1640 (Biosharp, Beijing Labgic Technology, China) + 10% FBS (10091148, Gibco, New York, USA) + 10000 U/mL penicillin and 10000 μg/mL streptomycin (sv30010, Hyclone, Utah, USA). Two culture models were performed in this research: (1) monoculture: KG-1a cells or BMSCs cells were respectively cultured in 25 cm [2] flasks. (2) coculture: KG-1a and BMSCs were suspended in RPMI 1640 (without FBS) and seeded a 6-well plate.

Cell sorting

According to BMSCs did not express CD45 [20] while KG-1a expressed high CD45 [21]. After 48 h coculture of KG-1a cells and BMSCs, the suspension of cells was added with CD45$^+$magnetic beads (100–0105, Stemcell, Vancouver, Canada). Following the manufacturer's instructions, CD45$^+$ KG-1a cells and CD45$^-$ BMSCs were separated with the help of a magnetic MACS separator. Apoptosis was assessed by flow cytometry.

Overexpression of CX43 in BMSCs

BMSCs were transfected with CX43 overexpression lentivirus or empty vector (purchased from Oligobio, Beijing, China) under the favor of polybrene following the manufacturer instructions. After 72–96 h of transfecting, 2 μg/mL puromycin (P8230, solarbio, Beijing, China) was used for selecting cells. The overexpression level of CX43 was tested by Immunofluorescence, qRT-PCR, and Western blotting. The anti-CX43 antibody (ab11370) and anti-GAPDH antibody (AF2823) were purchased from Abcam and BeyoTime. Primers in qRT-PCR for CX43 are Forward-CAATCTCTCATGTGCGCTTCT and Reverse-GGCAACCTTGAGTTCTTCCTCT. Primers for GAPDH are Forward-GTCGGAGTCAACGGATTTG and Reverse-TGGGTGGAATCATATTGGAA.

Mitochondrial transfer tracking

MitoTracker™ Red FM (Molecular Probes; M22425, ThermoFisher, MA, USA) was used to label mitochondria. KG-1a cells or BMSCs were incubated with 200 nM MitoTracker Red in respective media at 37 °C for 10 min. After culture for 24 h, mitochondria-stained cells were seeded as monoculture or coculture. The cells were cultured for 48 h, they were fixed with 4% paraformaldehyde (PFA). For actin staining, the cells were incubated with 50 μg/mL of rhodamine phalloidin-iFiuor AF488 (ab176753, Abcam, Cambridge, USA) and incubated at room temperature for 2 h. For nuclear staining, the cells were incubated with 1 μg/ml DAPI (Beyotime, Beijing, China) for 15–20 min. Images were acquired on the Olympus IX73 (Olympus, Tokyo, Japan) or a laser scanning confocal microscope (Leica STELLARIS 5).

Cell cycle measure assay

The cell cycle assay was performed using a cell cycle and apoptosis kit (Beyotime, C1052). Cells were seeded at 100×10^4 cells/well (six-well plate) and cultured for 24 h with treatment of Cinobufagin. Subsequently, cells were fixed for 24 h at 4°C in pre-cooled 70% ethanol. Cells were stained with PI and analyzed by flow cytometry (BD FACS Calibur) for cell cycle.

EdU assay

10 nM EdU solution was added to the suspension of the plate, which was filled with BMSCs and KG-1a (1:2) coculture for 48 h in a 48-well plate. Detection of EdU was conducted under the protocol provided by the manufacturers (C0075S, Beyotime, Beijing, China). The EdU-positive cells were captured with a fluorescence microscope (Olympus, Tokyo, Japan).

Colony-forming unit assays

KG-1a cells (monoculture or coculture) were seeded in 6-well plates with 2 mL of methylcellulose (04100, Stemcell, Vancouver, Canada). 2 mL RPMI 1640+10% FBS was added after the methylcellulose was coagulated. The medium was changed twice per week. 15 days later, representative views were photographed, the average number of colonies per well was recorded, and colony formation was then assessed.

Seahorse extracellular flux analysis

To measure cellular metabolism in real-time, the XFe8 extracellular flux analyzer (Agilent Technologies, California, USA) was used to perform the Seahorse Mito Stress Test. The measurements were performed as the manufacturer's instructions. For BMSC cells, 0.01×10^6 cells were seeded into XFe8-well Seahorse microplates in respective media, which allowed the adhesion of cells overnight. On the experiment day, the media was replaced by the XF base medium (Agilent) supplemented with glucose, sodium pyruvate, and l-glutamine, after seeding the plate was equilibrated at 37 °C in an incubator without CO_2 for 1 h to reach the ideal pH of 7.4. For KG-1a cells, 0.02×10^6 cells were seeded onto poly-d-lysin-treated (ScienCell, San Diego California, USA) XFe8-well Seahorse microplates, allowing the adhesion of cells for 1 h with the supplemented XF base medium mentioned above. The Standard Mito Stress Test was performed with the stepwise injection of oligomycin, carbonyl cyanide p-trifluoromethoxy-phenylhydrazone (FCCP), and a mixture of rotenone and antimycin A, to measure oxygen consumption rate (OCR). Seahorse data was analyzed using Wave Software, and further analyzed in R Studio.

Metabolite detection and data analysis

The KG-1a cells were harvested after coculture with BMSCs or monoculture for 48 h. Seven biological replicates were utilized per treatment. Samples for the metabolomic analysis were prepared, and the bioinformatic analysis was performed by Shanghai Majorbio Co., Ltd. (http://www.majorbio.com/), following standard procedures. The metabolite extraction was used for LC/MS (Thermo Scientific, Vanquish Horizon system, USA; Thermo Scientific, Q-Exactive HF-X, USA) analysis. The data were analyzed through the free online platform of majorbio cloud platform (http://www.cloud.majorbio.com). The metabolites with VIP>1 and $p<0.05$ were identified as significantly differentiated metabolites.The MetaboLights study data in www.ebi.ac.uk/metabolights/MTBLS9445(MTBLS9445).

RNA sequencing and data analysis

RNA sequencing data of monoculture and coculture were compared to detect differentially expressed genes. The KG-1a cells were harvested after co-culture with BMSCs or monoculture for 48 h. Total RNA was extracted using TRIzol reagent (Thermo Fisher Scientific, 15596026)

according to the manufacturer's instructions. The RNA samples were then submitted to BGI Co., Ltd (Shenzhen, China) for transcriptome sequencing. The subsequent analysis and data mining was performed on Dr. Tom's Multiomics Data mining system (https://biosys.bgi.com). Gene ontology (GO) and KEGG pathway analysis. The RNA-seq data is stored in GEO(GSE254529).

Xenotransplantation

All procedures were approved by the Laboratory Animal Welfare and Ethics Committee of Chongqing University Cancer Hospital (approval number: CZLS20210691-A) and performed following ARRIVE(Animal Research: Reporting of in Vivo Experiments) guidelines 2.0. Twenty NOD/ShiLtJGpt-Prkdcem26ll2rgem26/Gpt mice (male, 20–25 g, 8 weeks) were obtained from GemPharmatech Co., Ltd, maintained in specific pathogen-free conditions in the Animal Experimental Center of the Chongqing University Cancer Hospital under a temperature- and humidity-controlled environment with alternating 12 h light/dark cycles with free access to food and water ad libitum. Animals received humane care which met the institutional guidelines for animal welfare.

Recipients were conditioned with 25 mg/kg busulfan (Abmole, M3356) one day before receiving KG-1a under different coculture in vitro. On the following day, mice were randomly divided into 4 groups as the KG-1a from different co-culture conditions: Co-BMSCs, Co-EV-BMSCs, Co-CX43-BMSCs, and Co-CX43-BMSCs + VCR. Subsequently, 3×10^6 KG-1a cells in 100μL PBS per mouse were injected via the tail vein. Mice were observed each day. Animals were euthanized with an inhalation of excess carbon dioxide after four weeks, bone marrow of mice was collected. Bone marrow cell morphology was assessed microscopically upon Wright-Giemsa staining (Baso, BA407). Flow cytometry was used to detect human CD45 (hCD45) and human CD34 (hCD34) positive cells in bone marrow to assess tumorigenic effects. Briefly, the bone marrow nucleated cells (BMNCs) are obtained after lysing the red blood cells using ACK Lysis Buffer (C3702, Beyotime, China), and stained with PE-conjugated anti-human CD45 (Biolegend, 304008) and APC-conjugated anti-human CD34 (Biolegend, 343510) antibodies. 7-AAD (BD, 559925) staining was used to exclude dead cells.Ten thousand precision count beads (BioLegend, 424902) were added to count cells. Flow cytometry was performed on the Gallios Flow Cytometer (Beckman, CytoFlexLX). A completed ARRIVE guidelines checklist is included in Checklist 1.

Statistical analysis

All the above data are means ± SD of three or more experiments. Samples were compared using ANOVAs and t-tests. $P<0.05$ ($^*P<0.05$, $^{**}P<0.01$) was the significance threshold. Statistical analysis was performed using Prism version 6.0 (GraphPad Software, La Jolla, CA, USA).

Results

CX43 overexpression on BMSCs promoted mitochondrial transfer to KG-1a cells

To deeper study the role of CX43 overexpression between on BMSCs in leukemic cells function, bone marrow from AML patients was collected, mononuclear cells were isolated by density gradient centrifugation, and the cells cultured in respective media as Fig. 1a showed. After BMSCs were cultured for 10 days, the morphology of BMSCs was detected to ensure BMSCs homogeneity (Suppl. Figure 1). BMSCs have the ability of stemness and could differentiate into osteoblasts and other cells. To make sure BMSCs were isolated, the third-generation BMSCs were stimulated differentiation to osteoblasts, adipocytes, and chondroblasts (Suppl. Figure 1b). After 4–5 generations of culturing, BMSCs were transduced with CX43 (Fig. 1a), which promoted the expression of CX43 efficiently, the cells were labeled as CX43-BMSCs. While BMSCs were transduced with the empty vector as BMSCs expressed lower CX43, those were labeled as EV-BMSCs. The cells with the level of CX43 expression were confirmed by real-time PCR and western blotting (Fig. 1b and c, Suppl. Figure 2).

KG-1a cells, with over 90% exhibiting the $CD34^+/CD38^-$ phenotype, share characteristics with LSCs and are hard to eliminate [22]. Previous studies suggest their similarity to LSCs in terms of differentiation, proliferation, and self-renewal [23]. To investigate the impact of BMSCs on the stemness of LSCs, we opted to co-culture the leukemia stem cell line KG-1a [24] with BMSCs. The mitochondria of BMSCs were labeled by MitoTracker Red, so mitochondria from BMSCs were stained as red ones. After 48 h of co-cultured BMSCs with KG-1a cells, the mean fluorescence intensity of mitochondria in KG-1a was measured under confocal microscopy. TNTs were enriched with F-actin [25] that was labeled, the mitochondria from CX43-BMSCs transferred to KG-1a were detected through TNTs (Fig. 1d). The intensity of mitochondria was significantly higher in co-cultured with CX43-BMSCs (Fig. 1d). With the help of CX43, mitochondria from BMSCs were transferred to LSCs efficiently improved. No surprise, KG-1a cells grew faster in co-cultured with CX43-BMSCs. Due to mitochondria, transferred from BMSCs, satisfied more energy need of LSCs, and supported the cell growth (Fig. 1f and g).

Vincristine (VCR) was a conventional chemotherapy drug in acute leukemia and other solid tumors [26], it also successfully disturbed the function of TNTs generation and decreased mitochondrial transport [27] that it was facilitated as the inhibitor of microtubules. Different concentrations of VCR were measured to guarantee

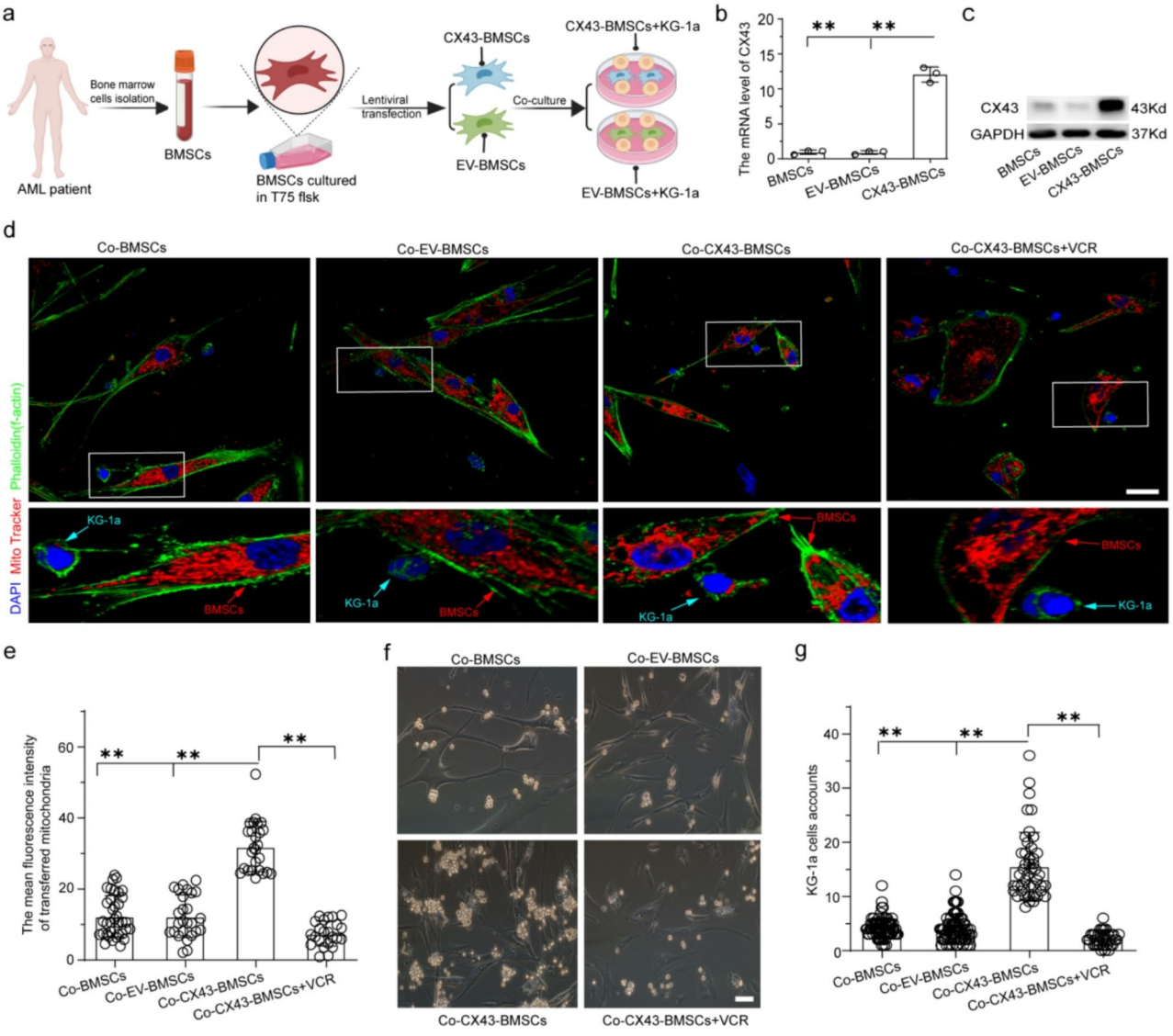

Fig. 1 Overexpression of CX43 promoted mitochondrial transfer from BMSCs to KG-1a cells. (**a**) Schematic illustration of establishing the CX43 overexpression model in bone marrow stromal cells. (**b**) Detection of CX43 mRNA expression in BMSCs with CX43 overexpressing lentivirus, or not. Values are presented as mean ± SD ($n = 3$). (**c**) Expression of the CX43 protein in BMSCs with CX43 overexpressing lentivirus. (**d**) Typical confocal microscope photos of KG-1a cells and BMSCs co-cultured 48 h without FBS. Mitochondria from BMSCs were labeled with Mitotracker Red(red); F-actin were labeled with Phalloidin 488 (Green), nuclei were labeled with DAPI 350 (blue). Scale bar, 25 μm. (**e**) The Average fluorescence intensity of KG-1a cells after co-cultured with BMSCs without FBS for 48 h ($n = 3$). (**f**) Representative images of adherent KG-1a and BMSCs after co-cultured 48 h without FBS. Scale bar, 50 μm. (**g**) The number of adherent KG-1a and BMSCs after co-cultured 48 h without FBS

that VCR did not influence the biological behavior of BMSCs and KG-1a, 0.5nmol VCR in cocultured cells was selected as both of KG-1a and BMSCs cells viability were more than 90% (Suppl. Figure 3). Deeper study presented this concentration was able to not damage the growth of cells but disturbed mitochondria transfered. When VCR was added in co-cultured CX43-BMSCs and KG-1a cells at the same time, the intensity of KG-1a mitochondria transported from BMSCs was descended (Fig. 1e), the mitochondrial transfer was directly associated with CX43 expression and TNTs function. Meanwhile, under the function of VCR, KG-1a growth was decreased as fewer mitochondria were transferred into (Fig. 1f and g). CX43 recruited more LSCs connected with nearby BMSCs and BMSCs transferred mitochondria to LSCs via CX43. LSCs gained more mitochondria, which were beneficial to LSCs proliferation.

CX43 overexpression on BMSCs maintained KG-1a cells stemness in vitro and vivo

KG-1a cells, which were isolated after co-culturing with CX43-BMSCs, met more S and G1 phases than the ones

that co-cultured with EV-BMSCs or from under VCR function with CX43-BMSCs (Fig. 2a and b). More KG-1a cells were under cell division and proliferation after more mitochondria were transferred into the cells. After co-culturing with CX43 overexpression BMSCs, KG-1a grew significantly faster than the control groups which was co-culturing with CX43 lower expression (Co-BMSCs, Co-EV-BMSCs, Co-CX43-BMSCs+VCR), under measurement by EdU assay (Fig. 2c and d). Furthermore, the clonal formation assay demonstrated that KG-1a, when co-cultured with CX43-overexpressing BMSCs, exhibited a higher colony formation compared to co-culture with less expression of CX43. (Figure 2e and f). Conclusively, CX43 overexpression in BMSCs was in favor of LSCs proliferation limitlessly.

Furthermore, the effect of CX43 overexpression in BMSCs on the maintenance of KG-1a stemness was investigated based on xenograft mouse models. KG-1a, derived from different co-culture conditions (Co-BMSCs, Co-EV-BMSCs, Co-CX43-BMSCs, and Co-CX43-BMSCs+VCR) were transplanted into immunodeficient mice. Four weeks later, bone marrow was collected for morphological examination and flow cytometric analysis to assess AML and the number of LSCs. KG-1a co-cultured with CX43-BMSCs induced obvious AML in mice, as evidenced by the presence of immature blast cells in the bone marrow, identified through Wright-Giemsa staining, while other groups primarily showed various stages of mature cells (Fig. 3a). Flow cytometry analysis showed that, compared to the Co-BMSCs and Co-EV-BMSCs groups, the Co-CX43-BMSCs group exhibited a significant increase in both the absolute count and proportion of $hCD45^+$ cells (AML cells) and $hCD34^+$ cells (LSCs) in bone marrow (Fig. 3b-c). The count and proportion of AML cells and LSCs in the Co-CX43-BMSCs+VCR group were significantly lower than in the Co-CX43-BMSCs group (Fig. 3b-c), suggesting that inhibiting mitochondrial transfer from BMSCs to KG-1a markedly suppressed KG-1a's tumorigenic potential and stemness maintenance. The above results suggest that CX43 overexpression in BMSCs promoted the stemness of LSCs and the development of AML in vivo.

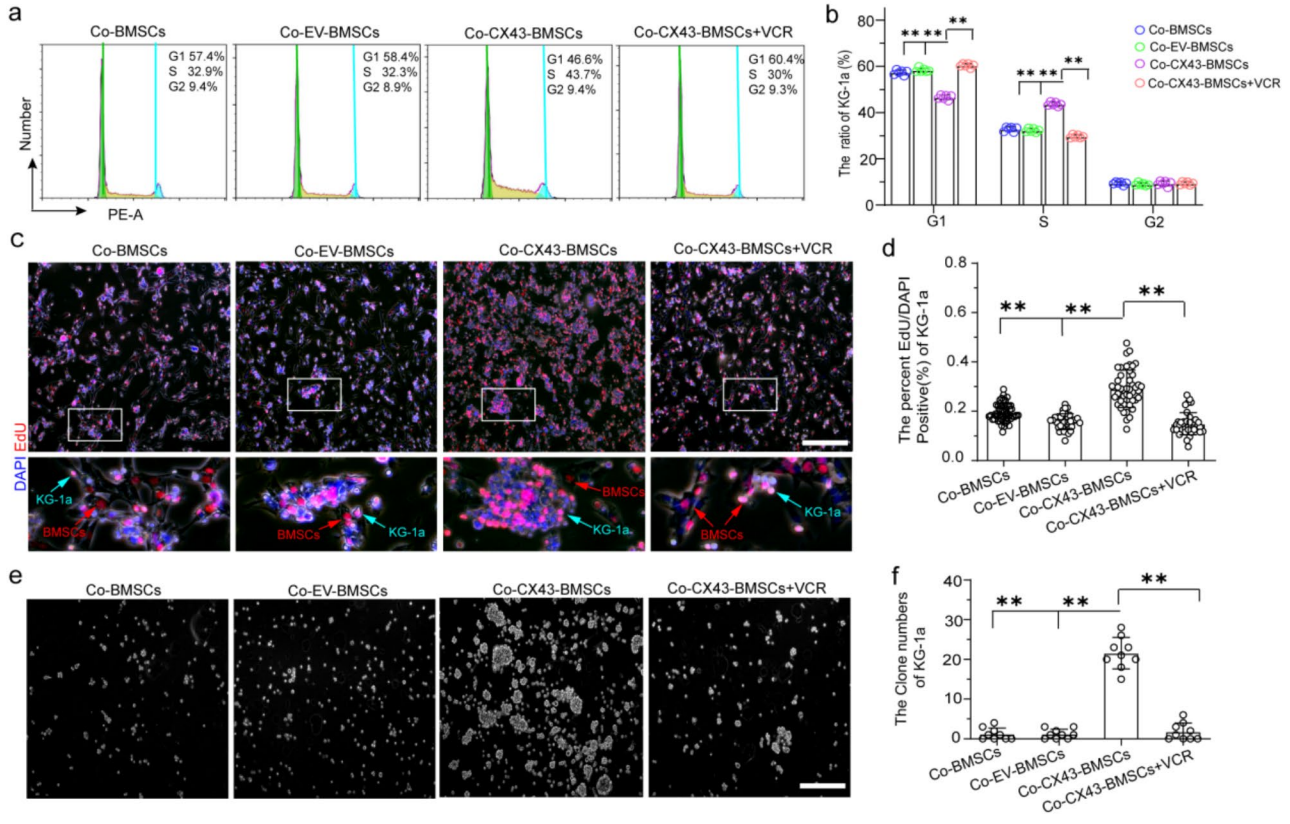

Fig. 2 Overexpression of CX43 increased the proliferation of co-cultured KG-1a. (**a**) Representative flow cytometric analysis of the cell cycle distribution in KG-1a cells isolated from co-cultured with BMSCs after 48 h without FBS was determined. (**b**) Quantification of periodic distribution in Fig. 2a. (**c**) Cell proliferation measured by EdU assay. Scale bar, 50 μm. (**d**) Quantification of the proliferation quantity of KG-1a cells in Fig. 2c. (**e**) Representative clone formation is shown. Scale bar, 50 μm. (**f**) Quantification of colony numbers in Fig. 2e

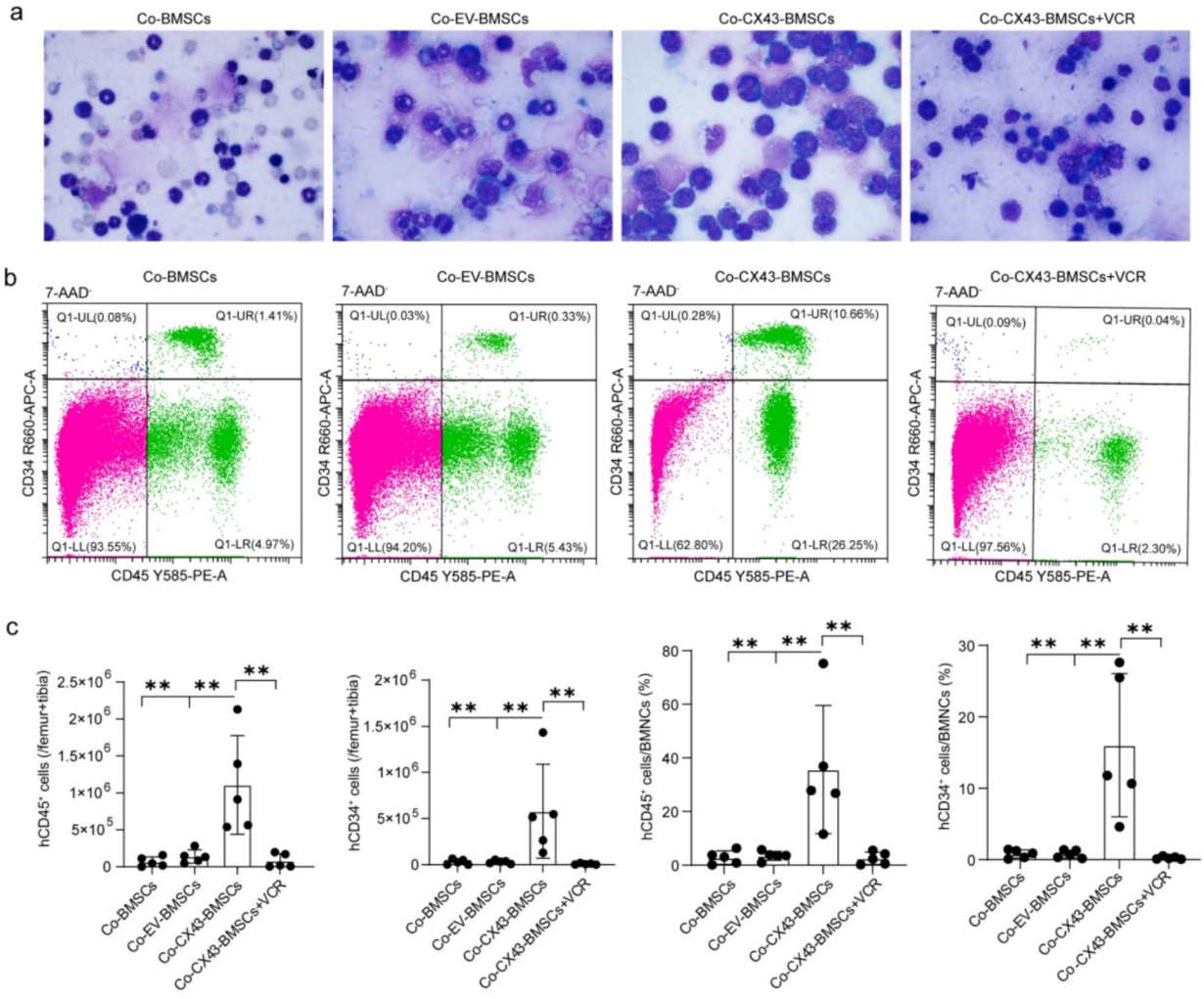

Fig. 3 Overexpression of CX43 in BMSCs promoted LSCs stemness and AML development in KG-1a xenograft mouse models. (**a**) Morphology of bone marrow cells from mice with Wright-Giemsa staining. (**b**) Representative flow cytometry analysis of $hCD45^+$ cells and $hCD34^+$ cells in bone marrow from mice. (**c**) The absolute count and proportion of $hCD45^+$ cells and $hCD34^+$ cells in bone marrow from mice. BMNCs: bone marrow nucleated cells. Data are presented as mean ± SD of 5 mice. $^{**}p < 0.01$

CX43 overexpression on BMSCs induced proliferation and adhesion related transcriptome signatures of co-cultured KG-1a cells

To detect the reason of LSCs growth unlimitly after co-culturing with CX43-BMSCs, RNA-seq was performed. Even 903 genes were expressed in both KG-1a cells that were co-cultured with CX43-BMSCs and EV-BMSCs, 81 genes were only highly expressed after co-cultured with CX43-BMSCs but not expressed after co-cultured with EV-BMSCs or KG-1a monocultured (Fig. 4a). The different gene distribution of KG-1a cells was deeper analyzed after co-cultured with CX43-BMSCs or EV-BMSCs. 1976 up-regulated genes and 279 down-regulated genes were related to KG-1a cells after co-culturing with CX-BMSCs compared with EV-BMSCs (Fig. 4b). GO and KEGG analysis both indicated that related genes, which were focused on cell adhesion, proliferation, and migration, were up-regulated in KG-1a cells after co-culturing with CX43-BMSCs (Fig. 4c and d). RNA-seq verified that BMSCs and LSCs contacted more closely under CX43, BMSCs had the chance to transfer mitochondria to LSCs to satisfy cell proliferation and adhesion needs.

CX43 overexpression on BMSCs enhanced mitochondrial energy metabolism in co-cultured KG-1a cells

Mitochondria was the main organelle for cell metabolism, especially was close to oxidant phosphorylation (OXPHOS). To explore if transferred mitochondria could be worked in LSCs. KG-1a, isolated from co-culturing with or without CX43-BMSCs or EV-BMSCs, cell metabolism was measured by seahorse assay. Oxygen consumption rate (OCR) was proportional to mitochondrial

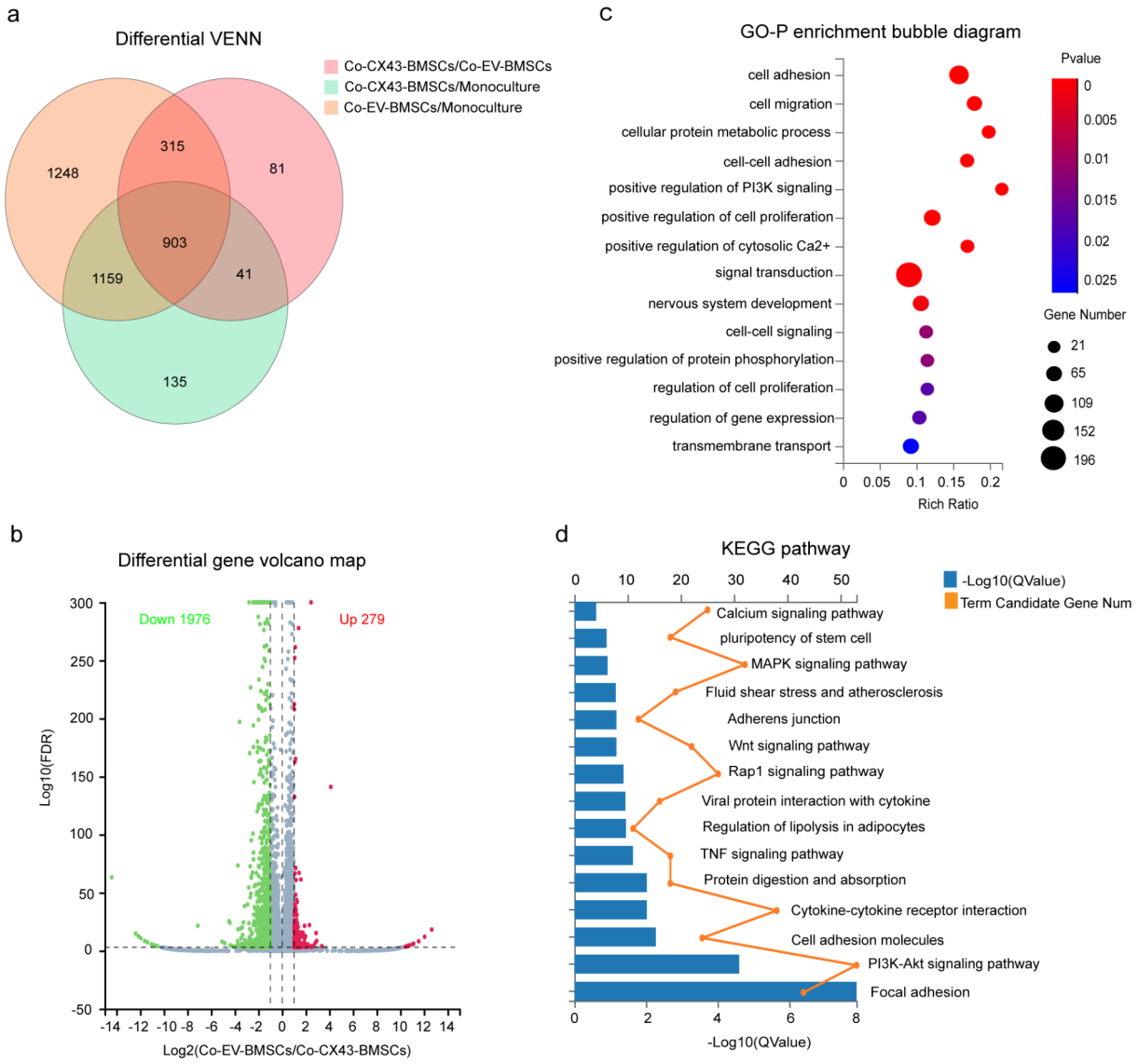

Fig. 4 Overexpression of CX43 promoted the proliferation and adhesion related transcriptome signatures of co-cultured KG-1a cells. (**a**) Venn diagram showing the number of gene distribution in KG-1a cells monocultured or co-cultured with BMSCs. (**b**) Scatter plots of differently expressed genes between KG-1a cells co-cultured with EV-BMSCs or CX43-BMSCs (false discovery rate (FDR) < 0.05). (**c**) GO analysis ($P < 0.0001$) of differently expressed genes from KG-1a cells which co-cultured with CX43-BMSCs or EV-BMSCs. (**d**) KEGG analysis of differentially expressed genes in KG-1a cells which co-cultured with CX43-BMSCs or EV-BMSCs. ($n = 3$)

respiration and recorded. The basal, maximal, and spare rate of OCR was much increased in KG-1a cells that come from co-cultured with CX43-BMSCs (Fig. 5a and b). Transferred mitochondria in KG-1a cells afforded energy for LSCs' unlimited division and proliferation. The OCR rate of BMSCs that were cultured separately was higher than the BMSCs that co-cultured with KG-1a cells (Fig. 5c and d). BMSCs owned more mitochondria originally and transferred mitochondria to LSCs under CX43.

CX43 overexpression on BMSCs drived metabolic reprogramming in co-cultured KG-1a cells

Metabolic reprogramming is closely linked to acute myeloid leukemia. To investigate how metabolic reprogramming unfolds within leukemic stem cells (LSCs) harboring augmented mitochondria, we conducted metabolite profiling following the transfer of mitochondria to KG-1a cells induced by CX43 overexpression in BMSCs. KG-1a cells were analyzed after being co-cultured with CX43-BMSCs or EV-BMSCs. the replicates were separately from different groups (Fig. 6a). The different metabolites from the two groups of KG-1a cells

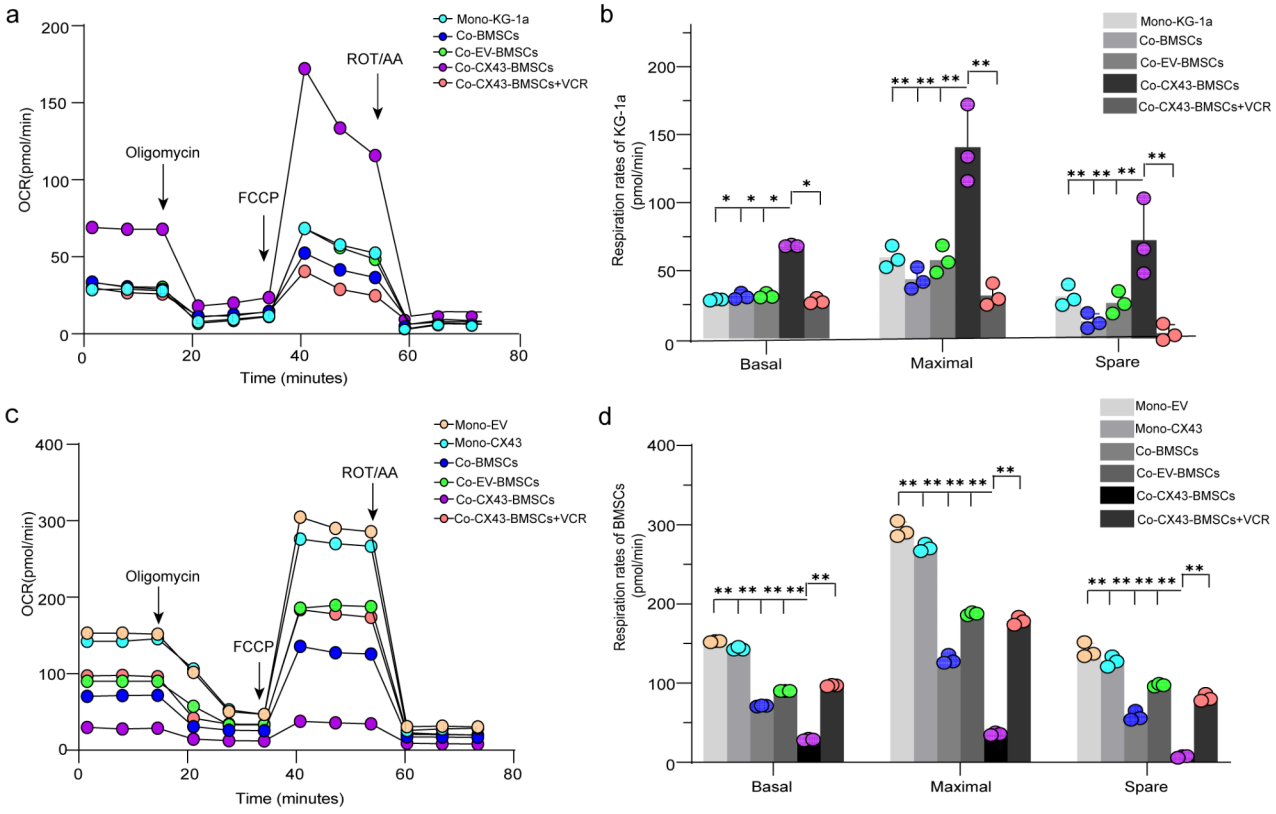

Fig. 5 Overexpression of CX43 increased the proliferation of cocultured KG-1a. (**a**, **b**) OCR of KG-1a cells monoculture or co-culture with BMSCs after 48 h without FBS. (**a**) basal, maximal and spare respiration. (**b**) of the indicated KG-1a cells ($n=3$). One-way ANOVA with Tukey's post-test. (**c**, **d**) OCR of BMSC cells monoculture or co-cultured with KG-1a cells for 48 h without FBS. (**c**) basal, maximal and spare respiration. (**d**) of the indicated BMSC cells ($n=3$). One-way ANOVA with Tukey's post-test. Values are presented as mean ± SEM ($n=3$)

which co-cultured with CX43-BMSCs and EV-BMSCs were mainly occupied by organic acids and derivatives, lipids and lipid-like molecules, organoheterocyclic, and nucleosides (Fig. 6b). Expression profile and KEGG analysis found that nucleoside metabolism was increased in KG-1a cells after co-culturing with CX43-BMSCs (Fig. 6c and d). AML with CX43 overexpression of BMSCs imposed nucleosides as fuel for cell metabolism.

Discussion

Chemotherapy was thought to eliminate the majority of bulk AML cells but not LSCs [11]. AML with relapsed/refractory (r/rAML) is thought to be lots of chemo-resistant residual LSCs located in bone marrow, which leads to AML progression and recurrence [28]. LSCs were verified to possess more energy metabolism [29]. LSCs are thought to cross-talk with bone marrow environment, which induces a conducive environment for leukemogenesis. In recent decades, much research found that BMSCs and LSCs have a very close connection with AML relapse and refractory, especially the way of mitochondria between LSCs and BMSCs. BMSCs transferred mitochondria to LSCs, which supplied additional organelle for LSCs and was inferior to AML patients. Karin and her colleagues once reported healthy hematopoietic stem and progenitor cells transferred mitochondria to BMSCs, which did a favor for BMSCs recovery [30]. Our previous study manifested BMSCs in AML cell lines were CX43 overexpression after receiving chemotherapy [16, 18, 31]. Our results indicate that CX43-mediated gap junctions and tunnel nanotubes contact BMSCs and LSCs cross-talk. Under CX43, mitochondria transfer between BMSCs and LSCs was improved, mitochondrial transfer of stem cell metabolic remodeling may improve anti-cancer efficacy and improve the overall survival of patients with AML. Further investigations thus seem warranted to provide a more comprehensive understanding of the metabolic remodeling in leukemia cells and the potential applications of chemotherapeutic agents.

With the help of CX43, the expression level of adhesion, migration, and proliferation-related genes in LSCs was increased. CX43 overexpression elevated the development of AML mice, which confirmed that CX43 worked for LSCs stemness in vitro and vivo. While VCR perturbed the mitochondria transport via impeding CX43, when VCR joined the co-culture of LSCs and BMSCs, the

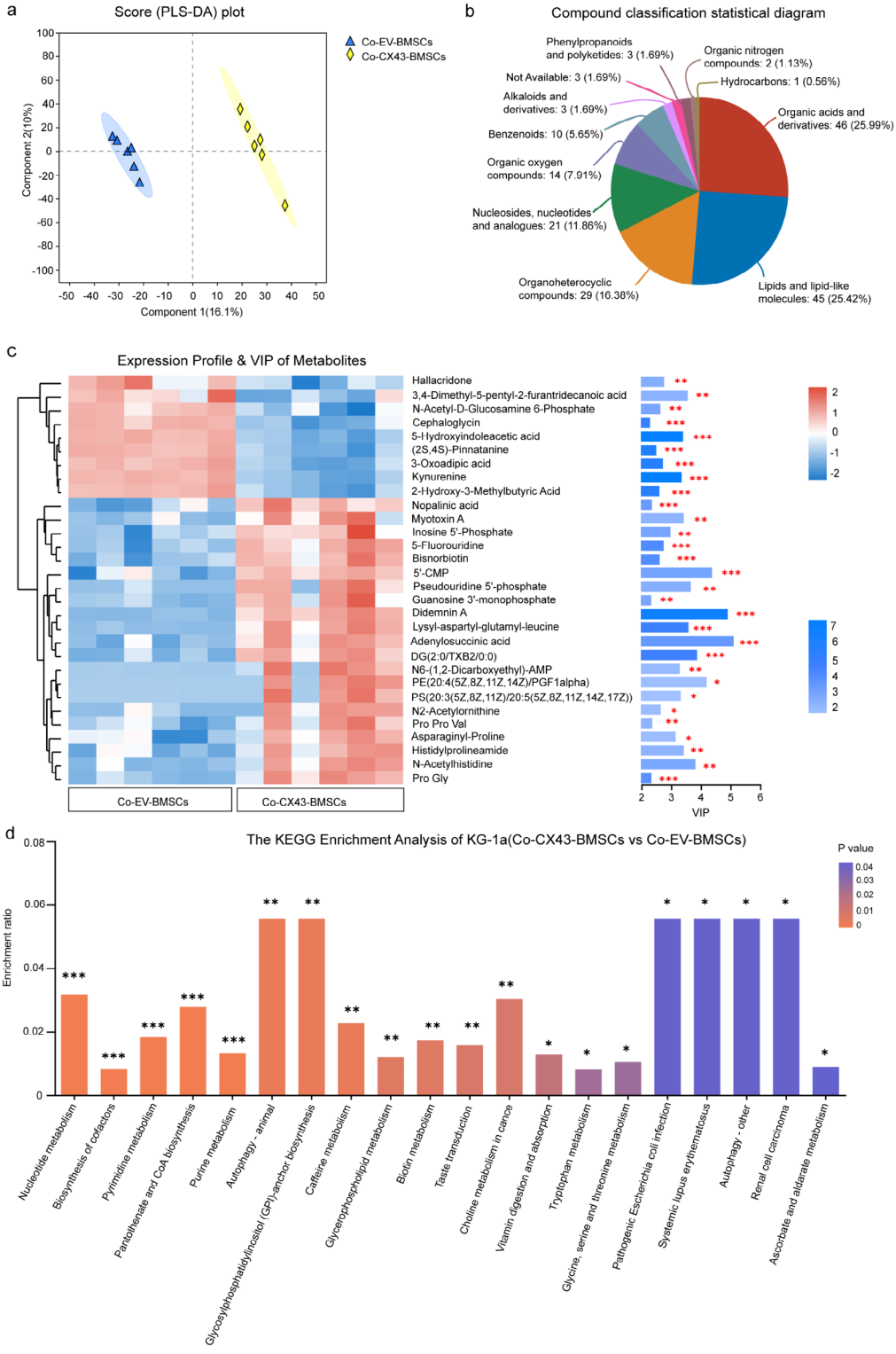

Fig. 6 Overexpression of CX43 promoted metabolic reprogramming in co-cultured. (**a**) The results from the PLS-DA demonstrated effective discrimination among the three groups. The X-axis represents the interpretation degree of Comp1's initial first predicted principal component, while the Y-axis represents the interpretation degree of orthogonal component 1's first orthogonal component. (**b**) The graph presents the names of the selected HMDB hierarchy (Superclass, Class or Subclass) and the percentage of metabolites they represent in descending order based on the number of metabolites. (**c**) Metabolite expression profile and VIP diagram. (**d**) KEGG enrichment analysis(Co-EV-BMSCs vs. Co-CX43-BMSCs)

stemness of LSCs was cut. LSCs recruited BMSCs nearby and attracted mitochondria from BMSCs transporting to the cells to imbalance the quiescence of LSCs. In addition, the main characteristic for LSCs to escape chemotherapy is to adhere to the BM niche directly [32]. More LSCs adhered to BMSCs with CX43 overexpression were found in the research, and as the CX43 expression level was reduced, the adhesion was less. CX43 could induce LSCs to adhere to BMSCs. As more mitochondria participated in LSCs, metabolic in LSCs altered.

Metabolic reprogramming occurred in numerous tumors, including AML. LSCs uptake amino acid or fatty oxidants as metabolic fuel and the level of OXPHOS was significantly increased [33, 34]. Biosynthesis metabolism contributed to chemo-resistant [35] and could be the novel therapeutic target to block leukemogenesis. Our data showed that biosynthesis metabolism was prior in LSCs after cocultured with CX43-BMSCs. The transfer was blocked by VCR directly, VCR enabled to disturb the function of TNTs, which was the composition of CX43. So CX43 played an important role in BMSCs and LSCs communication.

Our research has several noteworthy limitations. Our study focused on the mitochondrial transfer of BMSCs to LSCs in vitro, while no evidence revealed mitochondrial transfer to LSCs in vivo. Therefore, our further work will aim to understand mitochondrial transfer of BMSCs to LSCs in vivo and how they affect their physiological functions. Second, we confirmed the effect of mitochondrial transfer on BMSCs by various means in vitro. However, how to interfere with mitochondrial transfer in vivo to achieve targeted therapy for leukemia remains to be explored. Use the confirmed mechanisms of mitochondrial transfer to determine whether blocking mitochondrial transfer can reverse the metabolic reprogramming of leukemia and reduce the recurrence rate of leukemia caused by drug resistance.

Conclusions

In summary, our study explained CX43 was a connection between BMSCs and LSCs, providing a foundation for new therapeutic approaches exploiting CX43-enhanced mitochondrial transfer.

Supplementary Information

The online version contains supplementary material available at https://doi.org/10.1186/s13287-024-04079-3.

Supplementary Material 1

Supplementary Material 2

Acknowledgements
We express our gratitude to Zhian Hu for his insightful suggestions regarding this article and to Zhongjun Li for generously providing access to his experimental platform. The authors declare that artificial intelligence is not used in this study.

Author contributions
The study was conceived and designed by Zl.Y., Xm.Z., and Y.L. The experiments were performed by Hh.F. Data analysis was carried out by Xq.X. The manuscript was written by Hh.F. and Xq.X., and reviewed and revised by Zl.Y., Xm.Z., and Y.L. All authors have read and approved the final version of the manuscript for publication.

Funding
The study is partly supported by the National Natural Science Foundation of China (Grant No. 81670100, 82370114), Natural Science Foundation of Chongqing, China(2023NSCQ-MSX3235), and Fundamental Research Funds for the Central Universities, China(2023CDJYGRH-YB02).

Data availability
The materials supporting the conclusion of this research have been included in the article.

Data availability
The RNA-seq data is stored in GEO(GSE254529), and the MetaboLights study data in www.ebi.ac.uk/metabolights/MTBLS9445(MTBLS9445).

Declarations

Ethics approval and consent to participate
This study has been approved by the Research Ethics Committee of the Affiliated Cancer Hospital of Chongqing University. And informed consent was obtained from all subjects involvedin the study. The project was titled as "Effect and mechanism of GJIC mediated Rac1 protein inactivation to inhibit stemness of leukemia stem cells" approved on July 2017 (NO.81670100). The animal experimentswere in line with the regulations promulgated by The Laboratory Animal Welfare and Ethics Committee of the Affiliated Cancer Hospital of Chongqing University. The protocols for animal experiments adhere to the ARRIVE (Animal Research: Reporting of in Vivo Experiments) guidelines 2.0. The research project titled "CX43-mediated mitochondria transfer from bone marrow stromal cells promotes the stemness of leukemia stem cells" was approved on March 17, 2021 (CZLS20210691-A).

Conflict of interest
The authors declare that they have no competing interests.

Author details
[1]Department of Hematology Oncology, Chongqing Key Laboratory of Translational Research for Cancer Metastasis and Individualized Treatment, Chongqing University Cancer Hospital, Chongqing, China
[2]Department of Hematology, Chongqing, Central Laboratory, Chongqing University Fuling Hospital, Chongqing University Fuling Hospital, Chongqing, China

Received: 5 June 2024 / Accepted: 25 November 2024
Published online: 02 December 2024

References

1. Vago L, Gojo I. Immune escape and immunotherapy of acute myeloid leukemia. J Clin Invest. 2020;130:1552–64. https://doi.org/10.1172/jci129204.
2. Schlenk RF. Acute myeloid leukemia: introduction to a series highlighting progress and ongoing challenges. Haematologica. 2023;108:306–7. https://doi.org/10.3324/haematol.2022.280803.
3. De Kouchkovsky I, Abdul-Hay M. Acute myeloid leukemia: a comprehensive review and 2016 update. Blood Cancer J. 2016;6:e441–441. https://doi.org/10.1038/bcj.2016.50.
4. Yilmaz M, et al. Late relapse in acute myeloid leukemia (AML): clonal evolution or therapy-related leukemia? Blood Cancer J. 2019;9:7. https://doi.org/10.1038/s41408-019-0170-3.
5. DeWolf S, Tallman MS. How I treat relapsed or refractory AML. Blood. 2020;136:1023–32. https://doi.org/10.1182/blood.2019001982.

6. Naldini MM, et al. Longitudinal single-cell profiling of chemotherapy response in acute myeloid leukemia. Nat Commun. 2023;14:1285. https://doi.org/10.1038/s41467-023-36969-0.
7. Thomas D, Majeti R. Biology and relevance of human acute myeloid leukemia stem cells. Blood. 2017;129:1577–85. https://doi.org/10.1182/blood-2016-10-696054.
8. Basak GW, Srivastava AS, Malhotra R, Carrier E. Multiple myeloma bone marrow niche. Curr Pharm Biotechnol. 2009;10:345–6. https://doi.org/10.2174/138920109787847493.
9. Stone AP, Nascimento TF, Barrachina MN. The bone marrow niche from the inside out: how megakaryocytes are shaped by and shape hematopoiesis. Blood. 2022;139:483–91. https://doi.org/10.1182/blood.2021012827.
10. Jones CL, et al. Nicotinamide metabolism mediates resistance to Venetoclax in Relapsed Acute myeloid leukemia stem cells. Cell Stem Cell. 2020;27:748–e764744. https://doi.org/10.1016/j.stem.2020.07.021.
11. Jones CL, et al. Inhibition of amino acid metabolism selectively targets human leukemia stem cells. Cancer Cell. 2018;34:724–e740724. https://doi.org/10.1016/j.ccell.2018.10.005.
12. Lee KM, et al. MYC and MCL1 cooperatively promote chemotherapy-resistant breast Cancer stem cells via regulation of mitochondrial oxidative phosphorylation. Cell Metab. 2017;26:633–e647637. https://doi.org/10.1016/j.cmet.2017.09.009.
13. Forte D, et al. Bone marrow mesenchymal stem cells support Acute Myeloid Leukemia Bioenergetics and enhance antioxidant defense and escape from Chemotherapy. Cell Metab. 2020;32:829–e843829. https://doi.org/10.1016/j.cmet.2020.09.001.
14. Rosselló RA, Wang Z, Kizana E, Krebsbach PH, Kohn DH. Connexin 43 as a signaling platform for increasing the volume and spatial distribution of regenerated tissue. Proc Natl Acad Sci U S A. 2009;106:13219–24. https://doi.org/10.1073/pnas.0902622106.
15. Varela-Eirín M, et al. Extracellular vesicles enriched in connexin 43 promote a senescent phenotype in bone and synovial cells contributing to osteoarthritis progression. Cell Death Dis. 2022;13:681. https://doi.org/10.1038/s41419-022-05089-w.
16. Yang S, et al. Increased expression of CX43 on stromal cells promotes leukemia apoptosis. Oncotarget. 2015;6:44323–31. https://doi.org/10.18632/oncotarget.6249.
17. Chai C, et al. BCR-ABL1-driven exosome-miR130b-3p-mediated gap-junction Cx43 MSC intercellular communications imply therapies of leukemic subclonal evolution. Theranostics. 2023;13:3943–63. https://doi.org/10.7150/thno.83178.
18. Liu Y, et al. All-trans retinoic acid arrests cell cycle in leukemic bone marrow stromal cells by increasing intercellular communication through connexin 43-mediated gap junction. J Hematol Oncol. 2015;8:110. https://doi.org/10.1186/s13045-015-0212-7.
19. Islam MN, et al. Mitochondrial transfer from bone-marrow-derived stromal cells to pulmonary alveoli protects against acute lung injury. Nat Med. 2012;18:759–65. https://doi.org/10.1038/nm.2736.
20. Gao Q, et al. Bone marrow mesenchymal stromal cells: identification, classification, and differentiation. Front Cell Dev Biology. 2022;9. https://doi.org/10.3389/fcell.2021.787118.
21. Kamel AM, et al. Leukemia stem cell frequency at diagnosis correlates with Measurable/Minimal residual disease and impacts Survival in Adult Acute myeloid leukemia. Front Oncol. 2022;12. https://doi.org/10.3389/fonc.2022.867684.
22. Panyajai P, Tima S, Chiampanichayakul S, Anuchapreeda S. Dietary Turmeric Bisdemethoxycurcumin suppresses Wilms' Tumor 1 and CD34 protein expressions in KG-1a leukemic stem cells. Nutr Cancer. 2019;71:1189–200. https://doi.org/10.1080/01635581.2019.1598565.
23. She M, et al. Resistance of leukemic stem-like cells in AML cell line KG1a to natural killer cell-mediated cytotoxicity. Cancer Lett. 2012;318:173–9. https://doi.org/10.1016/j.canlet.2011.12.017.
24. Nirachonkul W, et al. CD123-Targeted Nano-Curcumin Molecule enhances cytotoxic efficacy in leukemic stem cells. Nanomaterials (Basel). 2021;11. https://doi.org/10.3390/nano11112974.
25. Tishchenko A, et al. Cx43 and Associated Cell Signaling pathways regulate tunneling nanotubes in breast Cancer cells. Cancers (Basel). 2020;12. https://doi.org/10.3390/cancers12102798.
26. Škubník J, Pavlíčková VS, Ruml T, Rimpelová S. Vincristine in Combination Therapy of Cancer: emerging trends in Clinics. Biology (Basel). 2021;10. https://doi.org/10.3390/biology10090849.
27. Allegra A, et al. Specialized Intercellular Communications via Tunnelling nanotubes in Acute and Chronic Leukemia. Cancers (Basel). 2022;14. https://doi.org/10.3390/cancers14030659.
28. Thakral D, Gupta R, Khan A. Leukemic stem cell signatures in Acute myeloid leukemia- targeting the guardians with novel approaches. Stem Cell Rev Rep. 2022;18:1756–73. https://doi.org/10.1007/s12015-022-10349-5.
29. Raffel S, et al. Quantitative proteomics reveals specific metabolic features of acute myeloid leukemia stem cells. Blood. 2020;136:1507–19. https://doi.org/10.1182/blood.2019003654.
30. Golan K, et al. Bone marrow regeneration requires mitochondrial transfer from donor Cx43-expressing hematopoietic progenitors to stroma. Blood. 2020;136:2607–19. https://doi.org/10.1182/blood.2020005399.
31. Liu Y, Zhang X, Li ZJ, Chen XH. Up-regulation of Cx43 expression and GJIC function in acute leukemia bone marrow stromal cells post-chemotherapy. Leuk Res. 2010;34:631–40. https://doi.org/10.1016/j.leukres.2009.10.013.
32. Tabe Y, Konopleva M. Role of Microenvironment in Resistance to Therapy in AML. Curr Hematol Malig Rep. 2015;10:96–103. https://doi.org/10.1007/s11899-015-0253-6.
33. Zhang YW, et al. GPRC5C drives branched-chain amino acid metabolism in leukemogenesis. Blood Adv. 2023;7:7525–38. https://doi.org/10.1182/bloodadvances.2023010460.
34. Han L et al. METTL16 drives leukemogenesis and leukemia stem cell self-renewal by reprogramming BCAA metabolism. Cell Stem Cell 30, 52–68.e13 (2023). https://doi.org/10.1016/j.stem.2022.12.006
35. Shi X, et al. Nuclear NAD(+) homeostasis governed by NMNAT1 prevents apoptosis of acute myeloid leukemia stem cells. Sci Adv. 2021;7. https://doi.org/10.1126/sciadv.abf3895.

Publisher's note